Available online at www.sciencedirect.com
ScienceDirect
International Journal of Mechanical Sciences 48 (2006) 1314–1322
International Journal of MECHANICAL SCIENCES
www.elsevier.com/locate/ijmecsci

Design, manufacture, and analysis of metal foam electrical resistance heater

Edward J. Cookson[a], Donald E. Floyd[a], Albert J. Shih[b,*]

[a]*Porvair Technical Center, Hendersonville, NC 28792, USA*
[b]*Department of Mechanical Engineering, University of Michigan, Ann Arbor, MI 48109, USA*

Received 5 January 2006; received in revised form 13 March 2006; accepted 13 May 2006
Available online 4 August 2006

Abstract

This paper presents a novel concept using the radial heating element made from porous Fe–Cr–Al metal foam in an air heater. Electrical resistance heating has been used extensively to convert the electrical energy into thermal energy. An analytic heat transfer model is first developed to estimate dimensions of the heating element. Four prototype Fe–Cr–Al metal foam electrical heaters with different levels of porosity and density are built. A more detailed computational fluid dynamics modeling of prototype heaters to include the temperature loss to the surroundings is developed. Experiments are conducted to evaluate the effects of airflow rates and electrical current and measure the change of air inlet and outlet temperatures. The experimental temperature measurements show reasonably good agreement with modeling predictions. Finally, improvements to the initial concept are discussed.

Keywords: Electrical resistance heating; Metal foam; Porous media

1. Introduction

Electrical resistance heating is a widely used technology to convert the electrical energy to thermal energy. The resistance to electrical current in a heating element generates heat, which is transferred to the air flowing through the heating element. This study investigates the use of open cell porous metal foam as the electrical resistant heating element.

An effective material for heating element must be electrically conductive with a high resistance. It also needs to be chemically stable to both oxidation and corrosion at high temperatures and has a high-melting point. Commonly used electrical resistance heating materials include the iron-based alloys (Fe–Cr–Al), nickel-based alloys (Ni–Cr), carbon compounds, cermets ($MoSi_2$), silicon carbide (SiC), tungsten, molybdenum, and platinum [1,2]. In this study, the Fe–Cr–Al alloy, also known as Fecralloy or Kanthal, is used as the material for metal foam heating element.

Four advantages of the porous metal foam electrical-resistant heater are: (i) light weight, (ii) low cost, (iii) adaptable to a cylindrical pipe and (iv) uniform heating of the whole volume of air flowing through the foam. Potential applications of this heating method include the household and office space heater and particulate filtration for diesel engine exhaust aftertreatment [3]. When a fine mesh porous metal foam is used, this device can be used for both filtration and heating. The filter can be self-cleaned by a process called regeneration, which is accomplished by passing a high electrical current flow through the metal foam-heating element to increase the metal foam temperature for burning the captured foreign particles.

In this study, a novel concept using the radial configuration of electrical current flow is proposed. The electrical current flows through a metal foam disk, which serves as the heating element, between an outside tube and an inner center rod. The configuration, material, and manufacture of the porous metal foam heater are first presented. The analytical method to design key dimensions of the metal foam heater is discussed. Results of more detailed modeling based on computational fluid dynamics using the FLUENT software are presented. Finally, experimental setup and testing results of the metal foam-heating device are

*Corresponding author. Tel.: +1 734 647 1766; fax: +1 734 936 0363.
E-mail address: shiha@umich.edu (A.J. Shih).

0020-7403/$ - see front matter © 2006 Elsevier Ltd. All rights reserved.
doi:10.1016/j.ijmecsci.2006.05.006

described and the comparison with modeling results is discussed.

2. Configuration and material of the metal foam heater

The following sections describe the design configuration, the metal foam material used, and the manufacture of metal foam heater.

2.1. Design overview

As shown in Fig. 1, the heating element is a thin metal foam disk inside a tube. Through the center of the metal foam disk is a cylindrical rod, which is electrically conductive and connected to the positive end of the DC electrical power supply. The negative end of the power supply is connected to the outside tube. Both the tube and rod are made of copper, a low electrical-resistivity metal. The electrical current flows from the center rod to the tube through the metal foam, which is made of high-temperature Fe–Cr–Al heating element alloy. Electrical resistance generates heat, which is carried away by the air flowing through the metal foam. Temperatures of the air before and after passing the heating element are measured using thermocouples, as shown in Fig. 1(a). One thermocouple measures the inlet air temperature, T_i, at a distance s_i from the edge of the metal foam. Two thermocouples measure the outlet air temperatures T_{o1} and T_{o2} with distance s_{o1} and s_{o2} from the other edge of the metal foam, respectively. All three thermocouples are placed close to the centerline of the tube. The radiation effect on temperature measurement is neglected due to the relatively low temperature, less than 125 °C, in this study. Outside the tube is a thermal insulation of thickness t. The width of the metal foam disk is denoted as w. The inner diameter of the tube and outer diameter of the rod is designated as D and d, respectively.

2.2. Foam material

The metal foam is made of Fe–Cr–Al alloy that can withstand operating temperatures in excess of 1200 °C. The open cell foam structure, as shown in scanning electron microscope micrographs in Fig. 2, consists of ligaments creating a network of inter-connected, dodecahedral-shaped cells [4]. The cells are randomly oriented and mostly uniform in size and shape. The ligament is hollow with a triangular-shaped hole, a result of the manufacturing technique used. The metal foams were produced using the open-cell polyurethane foam as templates [5,6]. The Fe–Cr–Al alloy powder slurry with Kelzan binder was coated to the polyurethane foam and fired in a vacuum furnace. The polyurethane foam was burned out during the firing, leaving the triangular-shaped hollow hole inside each of the ligaments.

Four Fe–Cr–Al metal foam-heating elements with two pore sizes and two weight densities are tested in this study. Two pore sizes are 80 and 100 ppi (pores per inch), which, as shown in Fig. 2, correspond to about 0.5–0.7 and 0.4–0.6 mm cell size, respectively. Two levels of density are 5 and 15 wt% relative to the density of a solid Fe–Cr–Al alloy.

The bulk Fe–Cr–Al alloy has an electrical resistivity of about 1.4 μΩ m [7]. In comparison, the copper and 316 stainless steel have electrical resistivities of 0.017 to 0.74 μΩ m, respectively. Since the metal foam is made of sintered powder, as well as highly porous, its electrical resistivity is much higher, and will vary with density. Electrical resistivity was measured for each of the Fe–Cr–Al foam used for prototype heaters. The measured electrical resistivity is listed in Table 1. The electrical resistivity of Fe–Cr–Al metal foam is much higher than the bulk Fe–Cr–Al alloy, about 20 times higher for the 15 wt% foam and 70 times higher for the 5 wt% foam. The high electrical resistance foam with 5 wt% can generate more heat per unit volume of heat element than the 15 wt% metal foam. This will be demonstrated later in experimental temperature measurements of different metal foam heaters. Table 1 also shows that, under the same wt%, the metal foam with larger cell size (80 ppi) has slightly higher overall electrical resistance than the foam with smaller cell size (100 ppi). This is possibly due to more dispersed ligaments in the metal foam with smaller cells.

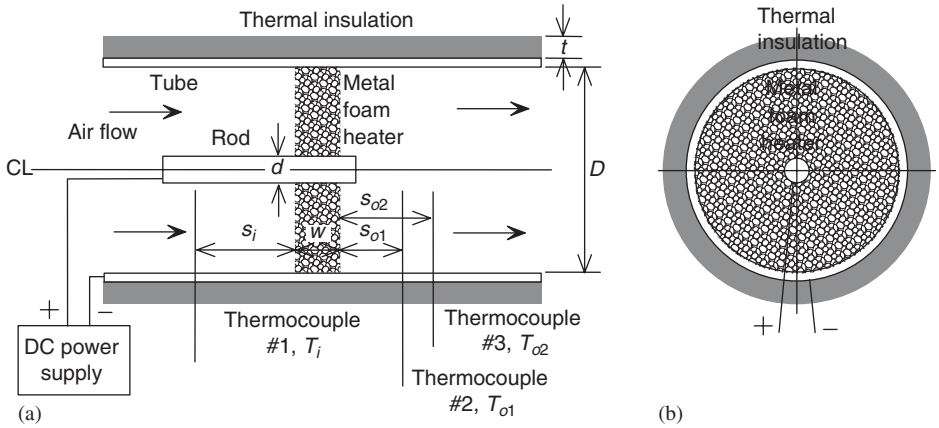

Fig. 1. Configuration of the metal foam electrical air heater. (a) Cross-section view and (b) axial view.

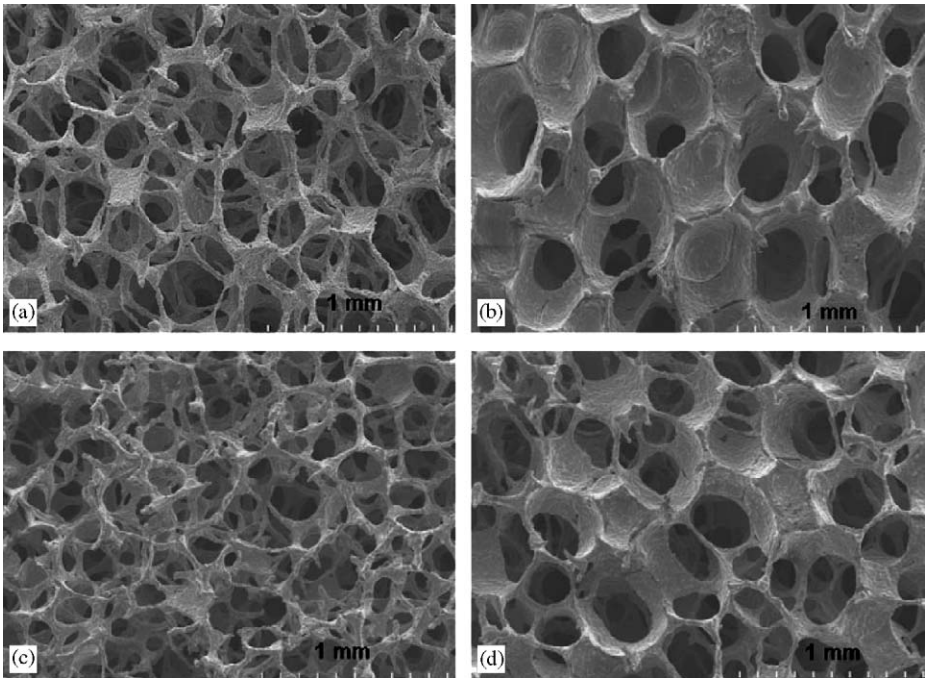

Fig. 2. SEM micrographs of (a) 100 ppi, 5 wt%, (b) 100 ppi, 15 wt%, (c) 80 ppi, 5 wt% and (d) 80 ppi 15 wt% Fe–Cr–Al metal foam.

Table 1
Electrical resistivity of four Fe–Cr–Al metal foams (μΩm).

	Weight density	
Porosity (%)	5	15
80 ppi	108	39
100 ppi	99.6	25

2.3. Brazing and assembly of the metal foam heating element

The Fe–Cr–Al foam is brazed to the copper tube and rod. The braze paste consists of, by weight, 5 parts BNi-6 braze powder, 1 part nickel metal powder, and 1 part Kelzan (xanthum gum) binder. The BNi-6 braze, composed of Ni with 11% P and 0.1% C, is chosen because it flows freely around the joint, binds well to Fe–Cr–Al alloy, and is suitable for use at elevated temperatures. During assembly, Ni wool is used to tighten the fit between the metal foam and the inner rod and outer tube. Dummy foam elements are inserted into the ends of the prototypes without braze paste to support the rod during the handling and firing. The green prototypes are fired in a vacuum furnace using the cycle shown in Table 2. Fig. 3 shows a circular metal foam disk cut by a core drill and the brazed metal foam heater. The residual Ni wool can be observed on the inside surface of the outer tube.

Table 2
Brazing cycle used to join the metal foam to the copper tube and rod

Segment	Ramp rate (°C/min)	Set point (°C)	Soak time (min)
1	8	121	10
2	6	943	5
3	1.5	971	30
4	Max	871	5
5	—	Room temp.	25

3. Dimensional design of metal foam electrical heater

The analytical method is developed to design the key dimensions of the metal foam-heating element and to estimate the temperature rise in the airflow.

The metal foam disk consists of a series of ring segments, as shown in Fig. 4. Each ring segment has the inside and outside radius of r_i and r_o, respectively. In the metal foam disk, the electrical resistance in the radial direction of a ring cross-section with distance r from the center is designated as R.

$$R = \rho \frac{\mathrm{d}r}{A}, \tag{1}$$

where ρ is the electrical resistivity of the metal foam, $A = 2\pi rw$ is the circumferential area of the ring.

Integrating for a ring of finite thickness from r_i to r_o, the inner and outer radii of the ring, the electrical resistance of the ring R_{ring} is derived.

$$R_{ring} = \int_{r_i}^{r_o} \rho \frac{\mathrm{d}r}{2\pi rw} = \frac{\rho}{2\pi w} \ln\left(\frac{r_o}{r_i}\right). \tag{2}$$

Since the ring segment is usually very thin, the area A of ring segment can be approximated by $\pi(r_o + r_i)w$ and the

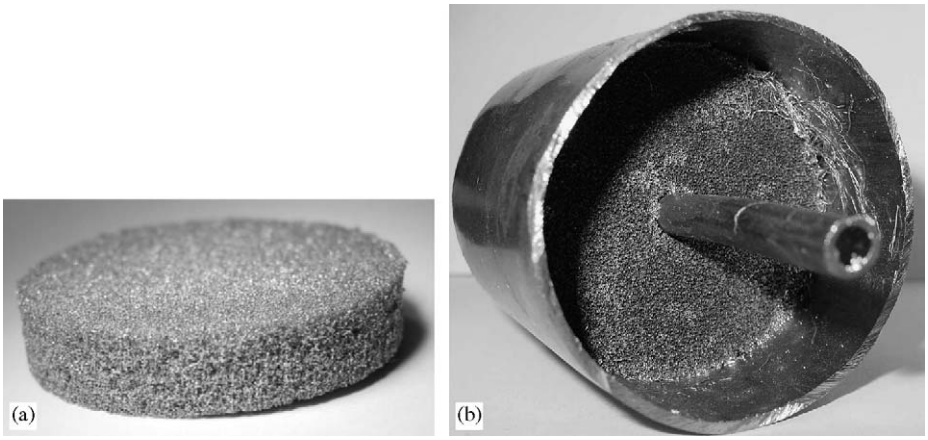

Fig. 3. Pictures of the (a) disk metal foam heating element (prior to the core drilling of center hole) and (b) brazed metal foam heating device with the Ni wool on the inner surface of the outer tube.

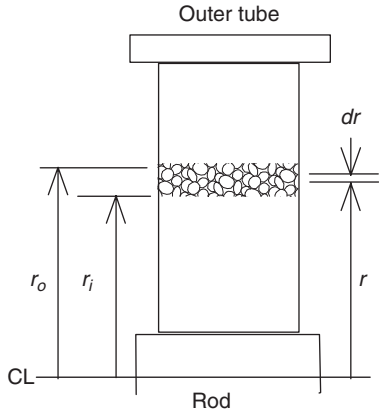

Fig. 4. A ring segment of metal foam in the disk-heating element used in analytical modeling.

R_{ring} can be expressed as

$$R_{ring} = \int_{r_i}^{r_o} \rho \frac{\mathrm{d}r}{\pi(r_o + r_i)w} = \frac{\rho(r_o - r_i)}{\pi w(r_o + r_i)}. \tag{3}$$

The summation of electrical resistant of ring segments made up the metal foam disk is the electrical resistance of the disk, R_{disk}, in the radial direction.

$$R_{disk} = \sum R_{ring}. \tag{4}$$

It is noted that, for a ring with the same width, the ring with larger radius on the outside of the disk has a smaller electrical resistance due to the increase in cross-sectional area for the electrical current flow. It is expected that more resistance heating and higher air temperature will therefore be generated in the inside ring segments.

The total heat generated in the disk by electric resistance heating, Q_{disk}, is calculated by

$$Q_{disk} = i^2 R_{disk}. \tag{5}$$

Part of the heat generated is lost through the insulation to the ambient environment. For cylindrical 1-D conduction, this heat loss, Q_{loss}, is given by [8]

$$Q_{loss} = \frac{2\pi(T_b - T_\infty)kl}{\ln((r_{ins} + t_{ins})/r_{ins})}, \tag{6}$$

where T_b is the temperature of the tube, T_∞ is the ambient temperature, k is the thermal conductivity of the insulation, l is the length of the cylinder, r_{ins} is the inner radius of the insulation, and t_{ins} is the thickness of the insulation. The tube has a thin wall thickness, relative to the inside diameter, and is made of high thermal conductivity material. In the cross-section perpendicular to the tube center axis, temperatures at inside and outside diameter of the tube are assumed to be the same.

The bulk temperature increase, ΔT, in the airflow across the metal foam-heating disk can be estimated by

$$\Delta T = \frac{Q_{disk} - Q_{loss}}{\dot{m} C_p}, \tag{7}$$

where $\dot{m}$ is the mass flow rate and C_p is the specific heat of the air.

An example is given here of a Fe–Cr–Al foam disk of $w = 13$ mm, inner diameter $d = 6.35$ mm to fit the inner rod, and outside diameter $D = 50.8$ mm to fit inside a tube. The measured electrical resistivity of 5 wt%, 100 ppi foam is 99.6 μΩm. As shown in Table 3, the disk is divided into seven ring segments; each ring has radial thickness of 6.35 mm. Using Eq. (2), the innermost ring with $r_i = 3.18$ mm and $r_o = 6.35$ mm has an electrical resistance of 845 μΩ. For the same ring, using Eq. (3), a resistance of 813 μΩ is calculated. In comparison, the outermost ring with $r_i = 22.23$ mm and $r_o = 25.40$ mm, the electrical resistant calculated using both Eqs. (2) and (3) is the same, 163 μΩ. This value is significantly lower than that of the innermost ring. For the entire heating disk, summing the electrical resistance of seven ring segments yields a total electrical resistance of 2.54 mΩ using Eq. (2) and 2.49 mΩ using Eq. (3). For a electrical current $i = 50$ A, about 6.23 W of heat is generated in the disk Fe–Cr–Al metal foam element. Assuming under the atmospheric pressure and a temperature of 27 °C and the air flow rate of 4 L/min,

Table 3
The seven ring segments with to model the heat generation in the Fe–Cr–Al metal foam heating element for 100 ppi and 5 wt% under 50 A electrical current ($w = 13$ mm)

Ring	r_i (mm)	r_o (mm)	Electrical resistance (μΩ) [from Eq. (2)]	Electrical resistance (μΩ) [from Eq. (3)]	Heat generation rate (kW/m^3)[a]
1	3.18	6.35	845	813	1650
2	6.35	9.53	495	488	590
3	9.53	12.70	351	349	300
4	12.70	15.88	272	271	180
5	15.88	19.05	222	222	120
6	19.05	22.23	188	188	88
7	22.23	25.40	163	163	66

[a]Based on $i = 50$ A and electrical resistance from Eq. (3).

which correspond to an $\dot{m}$ of 7.74×10^{-5} kg/s, and C_p of 1007 J/kgK [8], the temperature rise of the air, ΔT, is 79.9 °C based on Eq. (7). The outlet temperature is predicted to be 107 °C. This is assuming the adiabatic boundary condition on the outer tube surface, i.e., $Q_{loss} = 0$.

This temperature rise represents an ideal case of all electrical heat converts to thermal heat and all carries away by the air without any loss, i.e., the outer tube is adiabatic and no heat transfer to the inner rod. In real tests, some of the heat generated by the metal foam heater will be transferred through the outer tube and insulation as well as through the inner rod to the surroundings. According to the manufacturer, the thermal conductivity k of the fiberglass insulation is about 0.043 W/m-K. Assuming $r_{ins} = 25.4$ mm and $t_{ins} = 19$ mm (used in the experiment) and $T_b = 107$ °C, $T_\infty = 27$ °C, and $l = 380$ mm (the entire length of the heater pipe used in the experiment), the $Q_{loss} = 15.5$ W. This is higher than the 6.23 W generated by the metal foam-heating element, thus it is not possible. By reducing l to 39 mm (three times the width of the metal foam) and keeping all the other variables the same, the Q_{loss} is 1.6 W. Under such Q_{loss} and using Eq. (7), the bulk temperature increase in the airflow across the metal foam heating disk is 59.5 °C.

This example shows that using the analytical model to accurately predict the heat loss and temperature rise is difficult. More detailed computational thermal-fluid modeling and metal foam heater experiments need to be conducted to gain a better understanding of the performance of metal foam electrical heaters. These two approaches are discussed in the next two sections.

4. Numerical modeling of metal foam electrical heater

The FLUENT computational fluid dynamics (CFD) software v.6.0 is used for more detailed modeling of the metal foam heater. The example analyzed in the previous section using the 50.8 mm outside diameter, 6.35 mm inside diameter, 13 mm thick, and 100 ppi, 5 wt% Fe–Cr–Al foam heating element under 50 A electrical current and 4 L/min air flow rate is modeled for mutual comparison. Using the GAMBIT preprocessor, a model consisting of seven concentric rings listed in Table 3 is created to represent the metal foam. Circular cross-sections of the inlet and outlet with 50.8 mm outside diameter are also created to define a cylindrical shape control volume with the heating element inside. The 50.8 mm diameter outer surfaces (tube inside walls) are specified as walls, meaning that air cannot flow through them. The distance from the inlet and outlet cross-sectional surfaces to the metal foam is 100 mm. This length is long enough to allow close to the steady-state flow and temperature distributions to develop. The total length of the cylindrical control volume including inlet, foam, and outlet is 213 mm. It is noted that the inner rod is not included in the model of the inlet and outlet regions.

Fig. 5 shows the mesh used in the analysis. The heating element is broken into seven concentric cylindrical rings, each with a uniform heat generation rate, as listed in Table 3. Meshing is done by first paving the inlet cross-section surface of the heating element, and then expanding to a volume mesh using a Cooper mesh scheme [9]. Inlet and outlet zones are then meshed using the same manner, with the heating elements surface serving as the source for mesh generation. After meshing, properties of each surface and volume of the model are assigned. Porosity is assigned to the foam sections in the FLUENT solver.

The outlet air is assumed to be under uniform constant atmospheric pressure, since the heater outlet is open to ambient room conditions. The inlet cross-section is specified with a uniform velocity, V_{in}, which can be varied to correspond with the different flow rates by assuming uniform flow.

Three parameters, viscous resistance (R_{visc}), inertial resistance (R_{iner}), and porosity, are required in FLUENT to specify for the porous region for the metal foam heater. The viscous and inertial resistances for the metal foam with air as the working fluid have been tested at Porvair [10].

$$R_{visc} = 745400\rho_w^{2.06}e^{0.0364p^{0.63}}, \tag{8}$$

$$R_{iner} = 7.44\rho_w^{2.06}p^{0.63}, \tag{9}$$

where ρ_w is the percentage of weight density and p is the porosity of the foam in ppi.

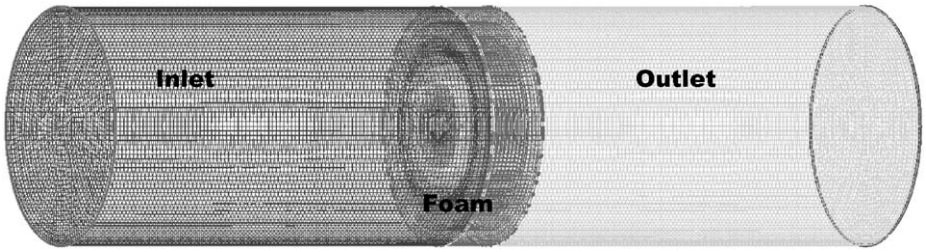

Fig. 5. Mesh of the metal foam heater with seven ring segments in the disk metal foam to model the heating generation in porous media in the metal foam heater.

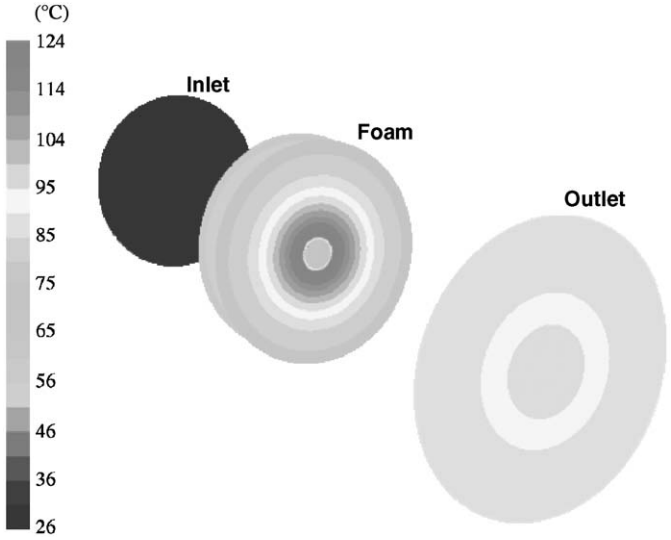

Fig. 6. Steady-state temperature profiles at the inlet entry and outlet exit surfaces and on the metal foam-heating element of the 100 ppi, 5 wt% density Fe–Cr–Al metal foam under 50 A current and 4 L/min flow rate, assuming adiabatic outer tube wall.

Outer wall of the heater was modeled as adiabatic insulation (zero heat flux). Results of temperature profiles for the 100 ppi, 5 wt% Fe–Cr–Al metal foam under 50 A electrical current heating, and 4 L/min air flow rate are shown in Fig. 6. In the inlet, the temperature is uniform at 27 °C. In the metal foam, during the higher electrical resistance and heater generation rate for inner ring segments, high temperature in the 114–124 °C range can be seen inside the metal foam disk. On the outside rings of the foam disk, the temperature drops to about 75–85 °C. In the exit surface of the outlet section, the air temperature ranging from 90 °C near the outside tube to 100 °C near the center axis is recorded. This value is slightly lower than the 107 °C of the uniform outlet temperature estimated in the analytical model. The error is possibly caused by the viscous and inertial resistance modeling in the flow model in Eqs. (8) and (9).

Fig. 7 shows two cross-sections of the temperature contours at a distance of 12.5 and 25.4 mm from the edge of the metal foam heater. For the cross-section close to the metal foam, as shown in Fig. 7(a), a high temperature gradient with 118 °C in the center to 75 °C near the outside tube can be seen. The fluid mixed and heat was transferred during the next 12.5 mm of travel. As shown in Fig. 7(b), a more uniform temperature distribution with 112 °C in the center and 69 °C near the outer tube can be observed.

By changing the boundary condition of the outer wall tube in the FLUENT modeling from adiabatic to radiation to 27 °C surroundings, the outlet air temperature at the cross-section 25.4 mm from the edge of the metal foam is reduced to a range of 49–100 °C. At the exit surface in the outlet, an average temperature rise of only 40 °C is estimated. This indicates that a significant Q_{loss} occurs in the current design. The experiment measurement in the next section will further verify this observation.

5. Experimental testing of prototype metal foam heaters

The design of experiments for metal foam heater, results from temperature measurement of the metal foam heater experiment, and discussion of the modeled and measured temperatures are presented.

5.1. Experimental design

The experimental metal foam heaters, as shown in Fig. 3, use a standard copper tube of 50.8 mm inside diameter and 1.5 mm wall thickness and a copper rod of 6.35 mm outside diameter. The width of the metal foam (w) is 13 mm. These dimensions match to those used in the analytical and numerical modeling. The total tube length is 380 mm, with the metal foam located in the center. Outside the tube, a layer of 19 mm thick fiberglass thermal insulation was used.

As discussed in Section 2.2, four heating elements are made of Fe–Cr–Al metal foam with 80 and 100 ppi porosity and 5% and 15% weight density. These metal foam-heating elements are brazed to the copper tube and rod to make the four heating devices for experimental testing.

The test configuration is shown in Fig. 1. A flow meter, Brooks Instrument 5850E, was used to control the volume of airflow rate through the metal foam-heating element. A DC power supply was used to generate the desired DC current through the heating element.

Two sets of experiment were conducted. One is a 5 h long-duration test using the 5 wt%, 100 ppi metal foam heater to study its characteristics for an extended period of

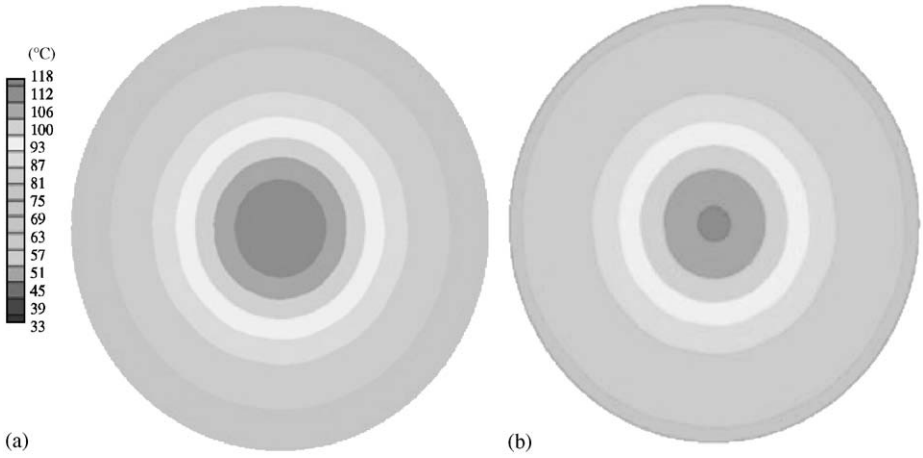

Fig. 7. Steady-state temperature profile at (a) 12.5 mm and (b) 25.4 mm from the edge of the 100 ppi, 5 wt% density Fe–Cr–Al metal foam under 50 A current and 4 L/min flow rate, assuming adiabatic outer tube wall.

time and to evaluate the time required to reach the steady-state heating condition. Another is a set of tests conducted on the four metal foam heaters. For each metal foam heater, four levels of air flow rate at 0.5, 1.0, 2.0, and 4.0 L/min and three levels of electrical current at 30, 40, and 50 A were tested. In total, 48 ($=4\times4\times3$) experiments were conducted.

The ambient, inlet, and averaged outlet temperatures were recorded during the all tests. As shown in Fig. 1, one inlet air temperature (T_{in}), two outlet air temperatures (T_{o1} and T_{o2}), and ambient room temperature (T_∞) are recorded using type K thermocouples. The distances s_i, s_{o1}, and s_{o2} are 200, 13, and 25 mm, respectively. The average of two outlet temperatures T_{o1} and T_{o2} is used to represent the average outlet air temperature, T_o. The averaging is done in real-time by the data-acquisition equipment.

5.2. Experimental results

5.2.1. Steady-state temperatures of a foam heater

Fig. 8 shows the inlet, ambient, and averaged outlet air temperatures recorded for 5 h. The ambient temperature starts at about 32 °C and gradually drops to 29 °C after 5 h. The test was conducted in a shop floor environment without precise temperature control, which results in such temperature fluctuation change. The inlet temperature, T_i, gradually increased from the ambient 32 °C to about 47 °C after 3 h of testing. The gradual increase in T_i is due to the heat conducted from the outer tube and inner rod to the front end of the heating device that pre-heats the inlet air. Following the trend of ambient temperature, T_i slightly dropped by about 2 °C from hour three to five. The average outlet temperature, T_o, also gradually increased to about 64 °C after 3 h. The difference of outlet and inlet temperature, ΔT, is also plotted in Fig. 8. The temperature rise reaches the steady-state condition of about 16 °C after about 20 min.

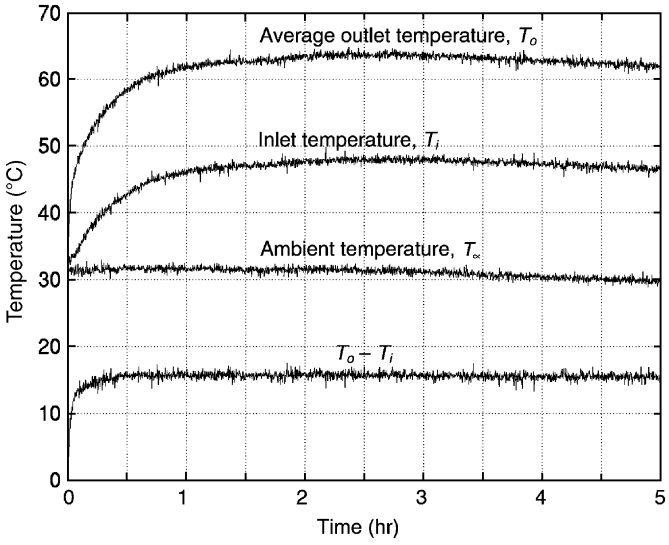

Fig. 8. Variation of the inlet, average outlet, and ambient temperature and the temperature rise across the metal foam for a 5-h long-duration test for the 5 wt%, 100 ppi Fe–Cr–Al foam under 50 A current and 4 L/min air flow rate.

5.2.2. Effects of air flow rate and electric current

Results of the temperature rise ($\Delta T = T_o - T_\infty$) of the 48 test conditions using 4 metal foam heating elements at 4 levels of air flow rate and 3 levels of electrical current flow after 20 min of heating are shown in Fig. 9. The 20 min is selected based on the results in Fig. 8. The temperature rise, $T_o - T_\infty$, is near the steady state after 20 min. The effects of electrical current, airflow rate, metal foam porosity (pore size), and wt% are studied.

The effect of electrical current on outlet temperature is as expected: when more electrical current is supplied to the metal foam heater, more heat is generated, and the temperature rise is greater. The effect of the airflow rate on temperature rise is not as obvious. As the airflow rate increases, the residence time of the air through the

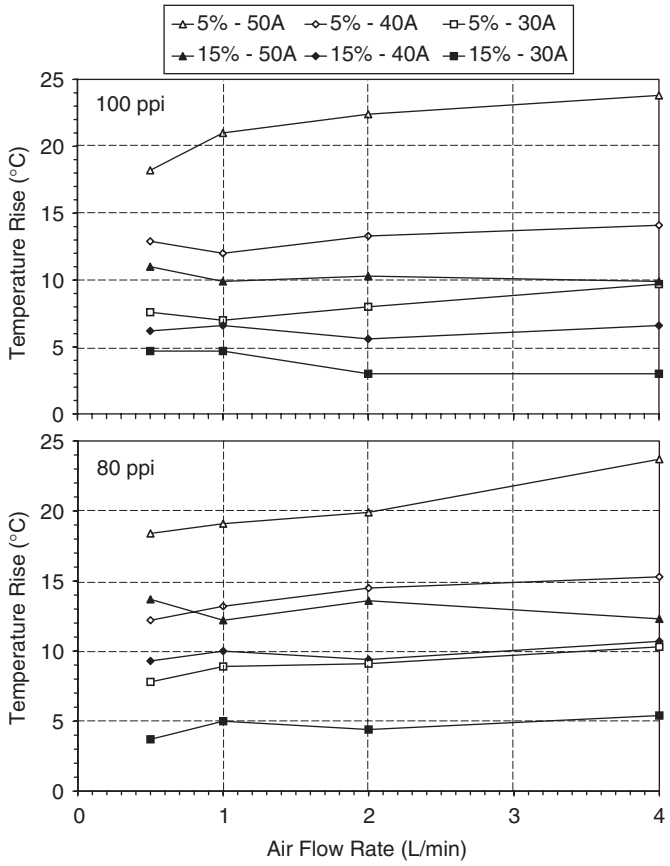

Fig. 9. Temperature rise of four Fe–Cr–Al metal foam heaters in the 48 heating tests after 20 min heating time.

heater is likewise decreased, which would lead to lower outlet temperatures. At the same time, however, the convective heat transfer coefficient increases, which would lead to more heat gain and higher temperatures [11,12]. Balance of the short residence time and high thermal convection can be seen in the mixed temperature rise results in Fig. 9. Detailed heat transfer and fluid flow analysis are necessary to explain the experimental results. This is a future research topic important for the device design.

The effect of the weight density of the metal foam on the temperature rise is obvious. As shown in Fig. 2 and Table 1, higher wt% foam has more metal and lower electrical resistivity. During electrical heating, less heat is generated and the temperature rise is lower. Fig. 9 indicates that 15 wt% metal foam heaters generate significantly less temperature rise than the 5 wt% metal foam heaters under the same testing conditions.

The porosity of the metal foam changes the electrical resistivity and the temperature rise. For the 5 wt% metal foam, as shown in Table 1, the change in porosity does not change much of the electrical resistance. The temperature rise of the 80 and 100 ppi metal foam heaters with 5 wt% density are about the same. For the 15 wt% Fe–Cr–Al metal foam, as shown in Table 1, the 80 ppi porosity metal foam has higher electrical resistance, which results in the greater temperature rise than the 100 ppi heater under the same testing condition.

5.3. Discussion

Compared to the CFD model prediction of 40 °C temperature rise, the experimental measurement of the steady-state temperature rise for the same 5 wt%, 100 ppi metal foam heater show about 33 °C, which is reasonably good agreement considering the complicated nature of the system. Compared to the analytical modeling with adiabatic boundary condition on the tube, the 80 °C temperature rise is much higher than the experimental measurement. This indicates that a significant portion of the heat is loss through the tube to the surroundings. In the design of the new metal foam heaters, such effect needs to be addressed.

6. Concluding remarks

In this study, a novel metal foam heater is studied. Four prototype metal foam heaters made of 80 and 100 ppi Fe–Cr–Al foam at 5 and 15 wt% were produced. Temperature rise of a metal foam heater for an extended period of time of heating test is studied to understand the time required to reach the steady-state heat transfer condition. Experiments were conducted using the four heaters at four levels of airflow rate and three levels of electrical current to investigate the temperature rise of the airflow through the metal foam. The computational fluid dynamics modeling of the metal foam heater showed reasonably good agreement with experimental measurement of the steady-state temperature rise in the 100 ppi, 5 wt% metal foam heater under 50 A electrical current and 4 L/min air flow rate.

It is possible to increase the resistance of the heating element by reducing its thickness. Reducing the width of the metal foam will increase the electrical resistance and

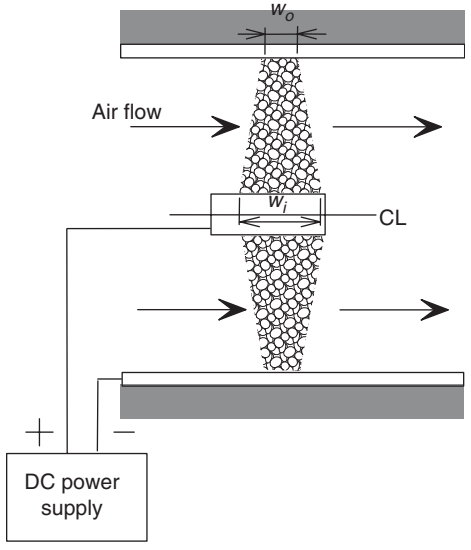

Fig. 10. The cross-section of a variable thickness metal foam-heating element.

raise the temperature of the metal foam. However, under a constant flow rate, residence time of the air in the foam is shortened. This could possibly reduce the heat transferred to the air. If thickness is decreased with increasing radius, a more uniform heat generation rate can be created. The variable thickness design of the metal foam disk is illustrated in Fig. 10. The width w_i of the metal foam disk in contact with the inner rod is wider than the width w_o on the outside of the disk. Turning the metal foam disk in a lathe is difficult. The cylindrical wire EDM process, as presented by [13,14], can be applied to manufacture the metal foam heater of such unique geometry.

References

[1] Hegbom T. Integrating electrical heating elements in appliance design. New York: Marcel Dekker; 1997.
[2] Erickson CJ. Handbook of electrical heating for industry. New York: IEEE Press; 1995.
[3] Yoro K, Itsauaki S, Saito H, Nakajima S, Okamoto S. Diesel particulate filter made of porous metal. Diesel exhaust aftertreatment, vol. 1313. Pennsylvania: SAE Special Publications, SAE Paper # 980187, SAE International; 1998. p. 17–23.
[4] Lu TJ, Stone HA, Ashby MF. Heat transfer in open-cell metal foams. Acta Materialia 1998;36:3619–35.
[5] Ashby M, Fleck NA, Hutchinson JW, Gibson LJ, Wadley H, Evans AG, Wadley HN. Metal foams—a design guide. London: Butterworth, Heinemann; 2000.
[6] Banhart J. Manufacture, characterization and application of cellular metals and metal foams. Progress in Material Science 2001;46: 559–632.
[7] Kanthal handbook—heating alloys for electric household appliances. Sweden: Kanthal AB; 2001.
[8] Incropera F, Dewitt D. Introduction to heat transfer. New York: Wiley; 2002.
[9] Blacker T. The Cooper tool. Fifth international meshing roundtable. New Mexico: Sandia National Laboratories; 1996. p. 13–30.
[10] Floyd D. Fluid properties of open cell sintered iron based porous metal structures, experimental results and discussion. Porvair Fuel Cell Technical Report, North Carolina, 2001.
[11] Calmidi VV, Mahajan RL. Forced convection in high porosity metal foams. Journal of Heat Transfer 2000;122:557–65.
[12] Hwang JJ, Hwang GJ, Yeh RH, Chao CH. Measurement of interstitial convective heat transfer and frictional drag for flow across metal foams. Journal of Heat Transfer 2002;124:120–9.
[13] Qu J, Shih AJ, Scattergood RO. Development of the cylindrical wire electrical discharge machining process: part I: concept, design, and material removal rate. Journal of Manufacturing Science and Engineering 2002;124:702–7.
[14] Qu J, Shih AJ, Scattergood RO. Development of the cylindrical wire electrical discharge machining process: part II: surface integrity and roundness. Journal of Manufacturing Science and Engineering 2002;124:708–14.